

2023

Section: Physics

Influence Of Cr⁺³ Ions Substitution On The Magnetic And Optical Properties Of Ni-Zn-Cr Ferrite/Pva/ Rhodamine Dye Nanocomposite Film

Ied M. Mnawer

Physics Department, Faculty of Science (Boys), Al-Azhar University, Nasr City, Cairo. Egypt

Osama M. Hemedda

Physics Department, Faculty of Science, Tanta University, Tanta, Egypt.

Mohamed Y. Hassaan

Physics Department, Faculty of Science (Boys), Al-Azhar University, Nasr City, Cairo. Egypt,
myhassaan@yahoo.com

Ahmed S. Abdel – Moety

Physics Department, Faculty of Science (Boys), Al-Azhar University, Nasr City, Cairo. Egypt

Mohamed M. Salem

Physics Department, Faculty of Science, Tanta University, Tanta, Egypt

Follow this and additional works at: <https://absb.researchcommons.org/journal>

How to Cite This Article

Mnawer, Ied M.; Hemedda, Osama M.; Hassaan, Mohamed Y.; Abdel – Moety, Ahmed S.; and Salem, Mohamed M. (2023) "Influence Of Cr⁺³ Ions Substitution On The Magnetic And Optical Properties Of Ni-Zn-Cr Ferrite/Pva/ Rhodamine Dye Nanocomposite Film," *Al-Azhar Bulletin of Science*: Vol. 34: Iss. 1, Article 9.

DOI: <https://doi.org/10.58675/2636-3305.1639>

This Original Article is brought to you for free and open access by Al-Azhar Bulletin of Science. It has been accepted for inclusion in Al-Azhar Bulletin of Science by an authorized editor of Al-Azhar Bulletin of Science. For more information, please contact kh_Mekheimer@azhar.edu.eg.

Influence of Cr^{+3} Ions Substitution on the Magnetic and Optical Properties of Ni–Zn–Cr Ferrite/PVA/Rhodamine Dye Nanocomposite Film

Ied Mohamed Mnawer^a, Osama Mohamed Hemedat^{a,b}, Mohamed Yousry Hassaan^{a,*}, Ahmed Saber Abdel-Moety^a, Mohamed Mostafa Salem^b

^a Physics Department, Faculty of Science (Boys), Al–Azhar University, Nasr City, Cairo, Egypt

^b Physics Department, Faculty of Science, Tanta University, Tanta, Egypt

Abstract

Nanocrystalline nickel-zinc substituted chromium ferrites having the chemical formula $\text{Ni}_{0.6}\text{Zn}_{0.4}\text{Cr}_x\text{Fe}_{2-x}\text{O}_4$, i.e., NZCrF (where $x = 0.0, 0.2, 0.4, 0.6, 0.8$ and 1.0 wt.%) have been synthesized by flash auto combustion method. Consequently, preparation and characterization of $\text{Ni}_{0.6}\text{Zn}_{0.4}\text{Cr}_{0.6}\text{Fe}_{1.4}\text{O}_4$ doped Polyvinyl alcohol (PVA)/Rhodamine dye nanocomposites using solvent casting technique have been reported. The X-ray diffraction (XRD) and Fourier-transform infrared spectroscopy (FTIR) studies confirm polymer nanocomposites' formation through the interaction between the nanoparticles and the polymer. Transmission electron microscope (TEM) and scanning electron microscope (SEM) images have investigated surface morphology and particle orientation. The average grain size is estimated to be approximately 51 nm. Images taken with TEM reveal that the composite $\text{Ni}_{0.6}\text{Zn}_{0.4}\text{Cr}_x\text{Fe}_{2-x}\text{O}_4/\text{PVA}$ morphology is highly agglomerated, suggesting magnetic nanoparticles are encased in the PVA polymer chains. This may be due to the interaction between the ferrite's oxygen atoms and the PVA's polymer chains. The saturation magnetization (M_s), remnant magnetization (M_r), and coercivity (H_c) measured by VSM have been studied. The modification of PVA/Rhodamine dye nanocomposites with $\text{Ni}_{0.6}\text{Zn}_{0.4}\text{Cr}_{0.6}\text{Fe}_{1.4}\text{O}_4$ reveals their potential for usage in luminescence applications due to an improvement in the composites' optical characteristics.

Keywords: Magnetic properties, Nanocomposites, Optical properties, PVA, Rhodamine dye, Spinel ferrite

1. Introduction

Spinel ferrites are economically significant materials due to their superior magnetic and electrical properties. Due to its potential electromagnetic properties at high frequency and low densification temperature, there has been an increase in interest in low-temperature sintered ferrites utilized as multilayer chip inductors [1]. For a long time, Ni–Zn ferrites have served as high-frequency ferrites for use in radio frequency (RF) coils, transformer cores, and antenna rods. Magnetic cores of reading/write heads for high-speed digital tape/disk recording use Ni–Zn ferrites with specific

properties, such as reduced porosity and regulated microstructure [2,3]. Pure ferrites' structural, electrical, and magnetic characteristics are altered when paramagnetic or diamagnetic ions (Cr^{3+} , Ni^{2+} , and Zn^{2+}) are substituted [4,5]. Impurities modify the crystal's defect structure and texture [6], affecting the material's magnetic and electrical characteristics in important ways. Cr-substituted ferrites have been the subject of a variety of scientific investigations. The magnetic, electrical, and structural features of ferrite have all been shown to change when Cr^{3+} ions are introduced. The magnetic characteristics and cation distribution of Cr-substituted ferrites prepared via an aerosol technique have been

Received 6 September 2022; revised 14 September 2022; accepted 15 September 2022.
Available online 13 October 2023

* Corresponding author. Fax: 0222629356.
E-mail address: myhassaan@yahoo.com (M.Y. Hassaan).

<https://doi.org/10.21608/2636-3305.1639>

2636-3305/© 2023, The Authors. Published by Al-Azhar university, Faculty of science. This is an open access article under the CC BY-NC-ND 4.0 Licence (<https://creativecommons.org/licenses/by-nc-nd/4.0/>).

investigated [7]. It has been observed that when the Cr-content rises, the saturation magnetization falls linearly. The antiferromagnetic characteristic of Cr^{3+} [8] was responsible for this discovery. As calcination temperature rises, pores are reduced, and grain size increases, leading to higher saturation magnetization [9–11]. Poly (vinyl alcohol) (PVA), obtained by saponifying poly (vinyl ether) or poly (vinyl ester), has garnered a lot of attention due to its usefulness and good features. In addition to its use as a scaffold for biosynthetic cartilage [12,13], PVA is also employed in wound dressings, catheters, contact lenses, and various other biomedical applications. Also, PVA stands out among polymers as a promising host material for different nanoparticles due to its large surface area, flexibility, and optical and mechanical characteristics [14,15]. Researchers have shown that low-dimensional materials exhibit high electron–hole recombination rates, high surface areas, and high activity for adsorption of UV–visible (VIS.) light [16]. Most industrial uses for Rhodamine dye [17] are in textiles, paints, paper, and biotechnology applications, including fluorescence microscopy and flow cytometry. The UV-VIS. spectroscopic absorption peak drops as the ferrite ratio rises, then rises again for NZCrF concentrations above $x = 0.3\%$. The PVA/Rhodamine dye combination is predicted to have an absorbance peak at 555 nm, and the absorbance of UV–visible light may be tuned by adjusting the ferrite ratio. The present work aims to develop a novel composite material with magnetic and optical properties. NiZnCr (NZCr) ferrite is synthesized by the flash auto-combustion technique substituted in PVA matrix doped with Rhodamine dye. Structural, morphological, magnetic, and optical properties are investigated for our prepared composite to be used in potential applications.

2. Experimental

2.1. Preparation of spinel ferrite ($\text{Ni}_{0.6}\text{Zn}_{0.4}\text{Cr}_x\text{Fe}_{2-x}\text{O}_4$)

Nanocrystalline nickel-zinc substituted chromium ferrites having the chemical formula $\text{Ni}_{0.6}\text{Zn}_{0.4}\text{Cr}_x\text{Fe}_{2-x}\text{O}_4$, i.e., NZCrF (where $x = 0.0, 0.2, 0.4, 0.6, 0.8$ and 1.0 wt.%) were prepared by flash auto-combustion technique using nickel-nitrate ($\text{Ni}(\text{NO}_3)_2 \cdot 6\text{H}_2\text{O}$), zinc-nitrate ($\text{Zn}(\text{NO}_3)_2 \cdot 6\text{H}_2\text{O}$), chromium-nitrate ($\text{Cr}(\text{NO}_3)_3 \cdot 9\text{H}_2\text{O}$), iron-nitrate ($\text{Fe}(\text{NO}_3)_3 \cdot 9\text{H}_2\text{O}$) as chemical reagents for synthesis, and urea $\text{CO}(\text{NH}_2)_2$ as a fuel. All chemicals are weighed according to comprehended compound ratios by knowing the stoichiometric ratio for each, then

250 mL distilled water is added and stirred for 20 min on a hot plate magnetic stirrer. The mixture is heated at 80°C with continual stirring until it becomes viscous, and then it is ignited internally until the solution becomes dry and reaches ash tree consistency. After that, the as-prepared powder was ground and left overnight at 100°C . To prevent any exterior phases, preliminary sintering was performed by annealing the powder to 600°C for 2 h at a rate of 5°C per minute.

2.2. Preparation of PVA/NZCrF composites by casting technique

Using the solution casting method, nano-composite PVA/NZCrF films are manufactured. Two hours of steady magnetic stirring at 90°C are used to dissolve 2000 mg of PVA in 50 mL of distilled water to produce a clear solution. For all composite samples with variable Cr-substitution (400 mg), NZCrF powder was added to the PVA solution and stirred at 90°C for 20 min with a magnetic stirrer to achieve a perfectly homogenous distribution of NZCrF particles inside the solution. The mixture of PVA and NZCrF is then cast into Petri plates and dried at room temperature. By the same technique, the nanocomposites thin film PVA/Rhodamine dye-doped with (0.1, 0.2, 0.3, 0.4, and 0.5 wt.%) of $\text{Ni}_{0.6}\text{Zn}_{0.4}\text{Cr}_{0.6}\text{Fe}_{1.4}\text{O}_4$ to enhance the optical properties of the prepared composite based on PVA/Rhodamine dye in the UV-VIS. light rang.

2.3. Characterization

Philips Model (PW–1729) diffractometer has been used to investigate the prepared materials by X-ray diffraction, while the samples were exposed to Cu-K_α radiation ($\lambda = 1.5411 \text{ \AA}$) at 300 K, 2θ operating between 10° and 80° to validate successful chemical reaction for the composites. Fourier transform infrared (FTIR) at room temperature in the range of 400 cm^{-1} to 4000 cm^{-1} with a resolution of 1 cm^{-1} was utilized to examine the chemical structure of composite materials. The morphology of composite ferrite samples is examined using a scanning electron microscope (SEM) (ZEISS Sigma 500 VP). To explore the nano-metric structure of the material, the transmission electron microscope (TEM) with 'JEM 2100 HRT'. The ferromagnetic hysteresis loop has been studied using a vibrating sample magnetometer (VSM; 9600–1 LDJ, USA) with an optimal applied field of 20 kG at room temperature. Using a UV–VIS. spectrophotometer, the optical characteristics of the produced samples

were measured in the range from 200 nm to 800 nm (Unicam spectrometer made in England).

3. Results and discussion

3.1. X-ray diffraction (XRD)

As shown in Fig. 1, the XRD patterns of PVA/NZCrF composite films produced at room temperature span the range $10^\circ \leq 2\theta \leq 80^\circ$. The PVA peak displays a diffraction peak at around $2\theta = 20^\circ$, which is attributable to the semi-crystalline character of PVA polymer molecules, which can come from strong intermolecular hydrogen bonding in the PVA chain while indicating the existence of a typical semi-crystalline nature [18]. Changing the NZCrF concentration in the PVA matrix does not affect the intensity of the primary peak at $2\theta = 19.5^\circ$, as the weight percentage (wt.%) of the doped ferrite in the PVA matrix remains constant at 16% for all composite samples with different Cr-substitution. As seen in Fig. 1, additional peaks corroborated that NZCrF was present in the PVA matrix. In addition, following doping, the XRD of PVA/NZCrF reveals other peaks. Doped ferrite samples are associated with reflections from the (220), (311), (400), (511), and (440) planes that correspond to the peaks.

3.2. Fourier transform infrared (FTIR)

As shown in (Fig. 2), infrared spectra of $\text{Ni}_{0.6}\text{Zn}_{0.4}\text{Cr}_x\text{Fe}_{2-x}\text{O}_4$ (where $x = 0.0, 0.2, 0.4, 0.6, 0.8,$ and 1.0 wt.%) were obtained in the region 400 cm^{-1} – 4000 cm^{-1} . All composite samples share the existence of the two primary absorption bands, ν_1 , and ν_2 , as indicated by the spectra. The lowest one (ν_1) is often recorded in the range 852 cm^{-1} and

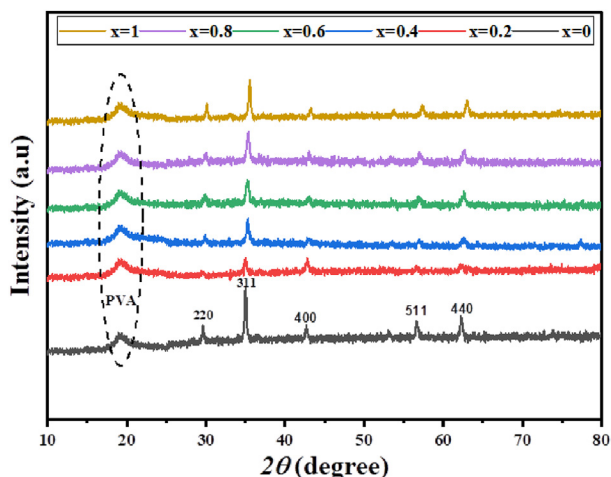


Fig. 1. XRD patterns of synthesized PVA/NZCrF composite films.

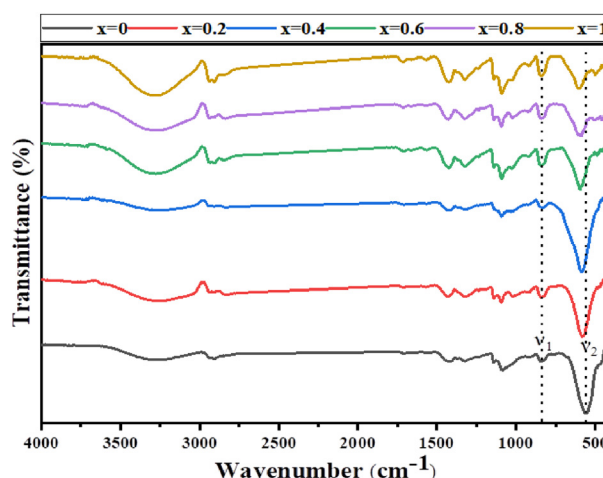


Fig. 2. FTIR spectra of synthesized PVA/NZCrF composite films.

corresponds to vibrations of the tetrahedral site, while the greatest one (ν_2) is typically observed in the range 503 cm^{-1} – 570 cm^{-1} and corresponds to vibrations of the octahedral site [19–21]. By increasing Cr-substitution, ν_2 shifts to a higher frequency, as seen in Fig. 2. Generally, the forecast of rising frequency for the ν_2 band implies that the band's force constant grows. The decrease in bond length causes the increase in force constant. Tetrahedral bonds almost remain constant by increasing Cr-substitution, whereas octahedral bonds vary. The shift of the ν_2 band is attributable to the depletion of octahedral bonds caused by a lack of Ni^{2+} ions. Due to hydroxyl groups (O–H) in the structure of all prepared PVA/NZCrF composite films, a wide-stretching vibration at about 3280 cm^{-1} has been detected. A faint band at around 2900 cm^{-1} corresponds to the stretching vibration of CH_2 , indicating the existence of PVA. In addition, 1460 cm^{-1} corresponds to the remaining water's H–O–H vibration and may be attributable to the stretching vibrations of the anti-symmetric NO_3^- , respectively. The band at 1090 cm^{-1} is attributed to the bond vibration between the oxygen ion and the tetrahedral metal ion ($\text{O}-\text{M}_{\text{tetra}}$) [1,22,23].

3.3. Scanning electron microscope (SEM)

As illustrated in Fig. 3, SEM is used to highlight surface morphology. The microscopy reveals that the average grain size is roughly 51 nm. The morphology seems irregular due to aggregation.

3.4. Transmission electron microscope (TEM)

The $\text{Ni}_{0.6}\text{Zn}_{0.4}\text{Cr}_x\text{Fe}_{2-x}\text{O}_4/\text{PVA}$ composite is heavily agglomerated in TEM images as in Fig. 4,

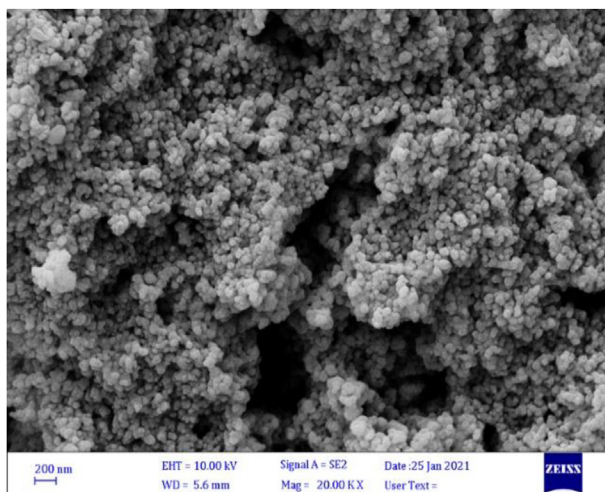


Fig. 3. SEM image of $Ni_{0.6}Zn_{0.4}Cr_{0.6}Fe_{1.4}O_4/PVA$ composites.

[25] indicating that nanocrystalline particles are surrounded by polymer chains of PVA, which may be a result of the interaction between oxygen atoms of ferrite and PVA. TEM images show that nanocrystalline particles are embedded in the PVA matrix with a core-shell configuration. PVA is an effective capping substance that plays a significant role in reducing the aggregation of nanoparticles, which is crucial for the dispersion and stability of ferrite particles [25]. The particle sizes were measured to be between 8.17 nm and 49.7 nm. The

increase in average particle size with increased Cr-concentration in ferrite may be attributed to the ferrite's embedding in the PVA matrix to form a core-shell structure.

3.5. VSM analysis

The composite magnetic hysteresis loops have been performed at room temperature for prepared PVA/NZCrF composite films using the VSM over the field range -20000 G to $+20000$ G, as shown in Fig. 5. The parameters obtained from these hysteresis loops (M_s), (M_r) and (H_c) are listed in Table 1, It can show from Fig. 6 that the changes in M_s , M_r , and H_c with adding NZCrF to PVA, where (M_s) changes from 0.19 emu/g to 14.97 emu/g, M_r changes from 0.07 emu/g to 1.78 emu/g, and H_c changes around 50.86 G to 132.65 G .

3.6. The impact of adding $Ni_{0.6}Zn_{0.4}Cr_{0.6}Fe_{1.4}O_4$ on the optical properties of PVA/Rhodamine dye nanocomposites

Each atom or molecule has a unique spectral response in Photoluminescence (PL) spectroscopy. Consequently, optical spectroscopy determines chemical substances' atomic or molecular structure and concentration. Fig. 7 shows the PL spectra for all investigated samples of nanocomposite thin film

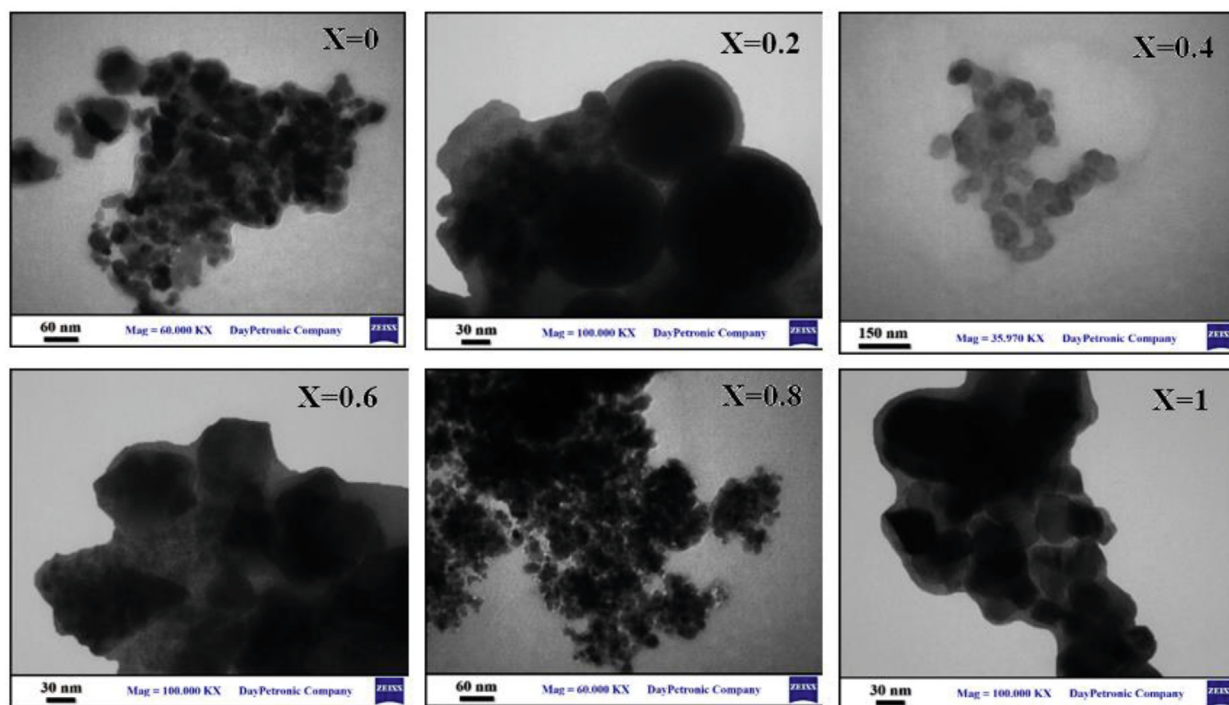


Fig. 4. TEM images of $Ni_{0.6}Zn_{0.4}Cr_xFe_{2-x}O_4/PVA$ composites.

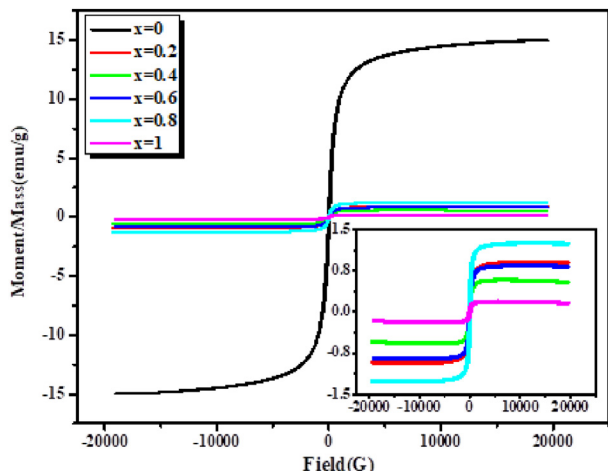


Fig. 5. Room-temperature hysteresis ($M-H$) loop of $Ni_{0.6}Zn_{0.4}Cr_xFe_{2-x}O_4/PVA$ thin film.

PVA/Rhodamine dye-doped with (0.1, 0.2, 0.3, 0.4, and 0.5 wt.%) of $Ni_{0.6}Zn_{0.4}Cr_{0.6}Fe_{1.4}O_4$. All samples were excited using laser light at a wavelength (360 nm) selected for the most efficient luminescence of Rhodamine dyes [25–27]. It illustrates the

Table 1. The saturation magnetization (M_s), remnant magnetization (M_r), and coercivity (H_c) of $Ni_{0.6}Zn_{0.4}Cr_xFe_{2-x}O_4/PVA$ thin film.

x	M_s (emu/g)	M_r (emu/g)	H_c (G)
0	14.978	1.7856	75.505
0.2	0.90296	0.0916	51.232
0.4	0.57784	0.0824	50.859
0.6	0.83838	0.1270	59.209
0.8	1.252	0.2585	62.991
1.0	0.19101	0.0708	132.65

PL spectra of the pure PVA, which display an extreme and broad emission band in the visible range at about (2.17 eV) and another peak at (2.41 and 3.05 eV); the former emission band is associated with surface trap-induced emission owing to the PVA capping. It was observed that for PL spectra of PVA/Rhodamine dye, there is a remarkable increase in the PL intensity. The main emission band shifted to a higher wavelength, exhibiting a well-known broadband emission around the green-yellow regions. The decrease in PL intensity with increased NZCr ferrite may be because of the clustering of nanoparticles at greater doping concentration, which reduces the interfacial area within the polymer and causes quenching [28,29]. This suggests that the composites are suitable for luminescence applications.

UV-VIS. Spectroscopy measures the optical absorption by atoms and molecules as a function of wavelength. As illustrated in Fig. 8. The absorbance peak decreases as the ratio of ferrite increases and then rises again when the NZCrF content exceeds $x = 0.3\%$. The absorbance peak of the composite containing Rhodamine dye is roughly identified at 555 nm, which is in excellent accord with the literature. Ferrite is expected to effectively decolorize Rhodamine dye between 60% and 70%. More donor energy and more oxygen vacancies contributed to the composite's increased deterioration. The effectiveness of nano ferrites as a catalyst is affected by the quantity of molecules present at the A and B-sites, which is another aspect that contributes to enhanced degradation efficiency. As they are separated from one another at the B-site,

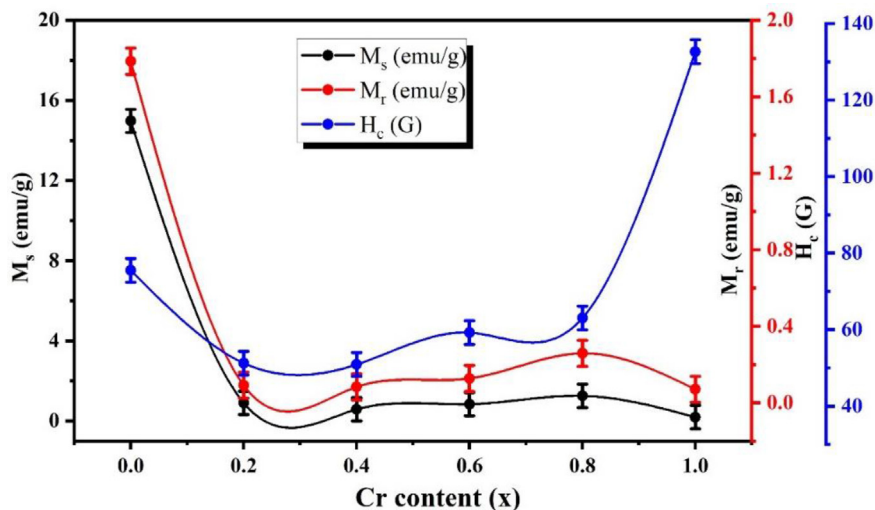


Fig. 6. The variation of the saturation magnetization (M_s), remnant magnetization (M_r), and the coercivity (H_c) of $Ni_{0.6}Zn_{0.4}Cr_xFe_{2-x}O_4/PVA$ thin film.

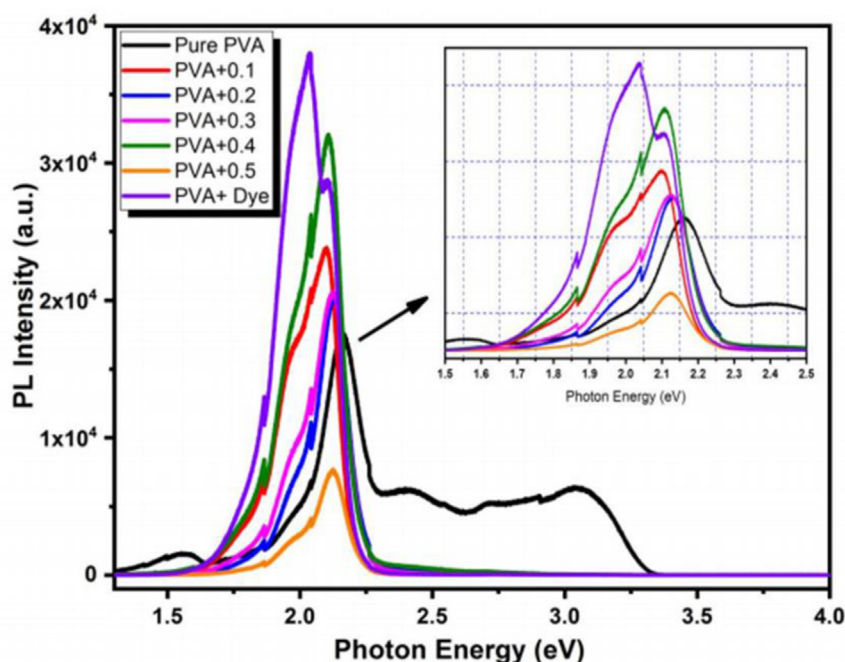


Fig. 7. PL spectra of nanocomposite thin film PVA/Rhodamine dye + different concentrations of $Ni_{0.6}Zn_{0.4}Cr_{0.6}Fe_{1.4}O_4$.

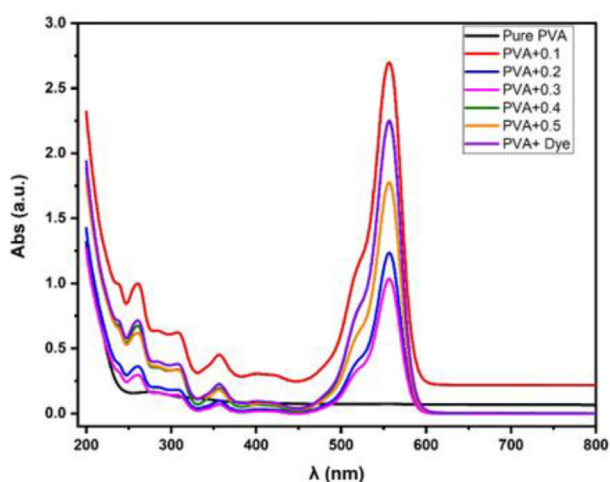


Fig. 8. UV-VIS. absorption spectrum of the investigated samples (PVA/Rhodamine dye) for different concentrations of $Ni_{0.6}Zn_{0.4}Cr_{0.6}Fe_{1.4}O_4$.

metal ions are conducive to photocatalytic action. The composite samples lose the transparency (decolorization) with adding darker ferrite the absorption of visible light increases consequently. The absorbance of UV-VIS. light can be optimized by changing the ferrite ratio in the PVA/Rhodamine dye matrix.

4. Conclusions

The flash auto combustion process was used to create nanocrystalline nickel-Zinc substituted

chromium ferrites with the chemical formula $Ni_{0.6}Zn_{0.4}Cr_xFe_{2-x}O_4$, or NZCrF (where $x = 0.0, 0.2, 0.4, 0.6, 0.8,$ and 1.0 wt.%). Nanocomposite PVA/NZCrF/Rhodamine films are fabricated utilizing the solution casting method. According to XRD, the PVA peak indicates a diffraction peak at approximately $2\theta = 20^\circ$, which is ascribed to the partially crystalline nature of PVA polymer, which can result from strong intermolecular hydrogen bonding along the PVA chain, despite the presence of a typical semi-crystalline nature. NZCrF infrared spectra reveal the existence of the two primary absorption bands ν_1 and ν_2 as a characteristic shared by all composite samples. The SEM estimates that the average grain size is around 51 nm. The morphology seems irregular due to aggregation. The NZCrF/PVA composite is heavily agglomerated in TEM micrographs, indicating that PVA polymer chains enclose ferrite particles may be a result of the interaction between the oxygen atoms of ferrite and PVA. The changes in M_s , M_r , and H_c are caused by the addition of NZCrF to PVA, where (M_s) changes from 0.19 emu/g to 14.97 emu/g, M_r changes from 0.07 emu/g to 1.78 emu/g, and H_c changes from approximately 50.86 G to 132.65 G. For PL spectra of PVA/Rhodamine dye, a significant rise in PL intensity and a shift in the main emission band to longer wavelengths were observed, exhibiting the well-known broad-spectrum emission in the green-yellow areas. The absorption peak (UV-VIS. spectroscopy) decreases with increasing ferrite ratio and subsequently increases with NZCrF concentrations above

$x = 0.3\%$. The composite, including Rhodamine dye, has an estimated absorbance peak of 555 nm and the absorbance of UV-VIS. light may be improved by varying the ferrite ratio in the PVA/Rhodamine dye matrix.

Conflicts of interest

The authors declare that they have no known competing financial interests or personal relationships that could have appeared to influence the work reported in this paper.

References

- [1] Yan S, Yin J, Zhou E. Study on the synthesis of NiZnCu ferrite nanoparticles by PVA sol-gel method and their magnetic properties. *J Alloys Compd* 2008;450:417–20.
- [2] Qian K, Yao Z, Lin H, Zhou J, Haidry AA, Qi T, et al. The influence of Nd substitution in Ni-Zn ferrites for the improved microwave absorption properties. *Ceram Int* 2020;46:227–35.
- [3] Thakur P, Taneja S, Chahar D, Ravelo B, Thakur A. Recent advances on synthesis, characterization and high frequency applications of Ni-Zn ferrite nanoparticles. *J Magn Magn Mater* 2021;530:167925.
- [4] Rezlescu E, Sachelarie L, Popa PD, Rezlescu N. Effect of substitution of divalent ions on the electrical and magnetic properties of Ni-Zn-Me ferrites. *IEEE Trans Magn* 2000;36:3962–7.
- [5] Patange SM, Shirsath SE, Toksha BG, Jadhav SS, Jadhav KM. Electrical and magnetic properties of Cr³⁺ substituted nanocrystalline nickel ferrite. *J Appl Phys* 2009;106:23914.
- [6] El-Sayed AM. Effect of chromium substitutions on some properties of NiZn ferrites. *Ceram Int* 2002;28:651–5.
- [7] Iqbal MJ, Ahmad Z, Meydan T, Nlebedim IC. Influence of Ni-Cr substitution on the magnetic and electric properties of magnesium ferrite nanomaterials. *Mater Res Bull* 2012;47:344–51.
- [8] El-Ghazzawy EH, Alamri SN. NiCr_xFe_{2-x}O₄ ferrite nanoparticles and their composites with polypyrrole: synthesis, characterization and magnetic properties. *Bull Mater Sci* 2015;38:915–24.
- [9] Li J, Li Y, Tian X, Zou L, Zhao X, Wang S, et al. The hardness and corrosion properties of trivalent chromium hard chromium. *Mater Sci Appl* 2017;8:1014–26.
- [10] Bi HY, Jiang XX, Li SZ. The corrosive wear behavior of Cr-Mn-N series casting stainless steel. *Wear* 1999;225:1043–9.
- [11] Huang CA, Lin CK, Yeh YH. Increasing the wear and corrosion resistance of magnesium alloy (AZ91D) with electrodeposition from eco-friendly copper-and trivalent chromium-plating baths. *Surf Coating Technol* 2010;205:139–45.
- [12] Fan J, Zhou W, Wang Q, Chu Z, Yang L, Yang L, et al. Structure dependence of water vapor permeation in polymer nanocomposite membranes investigated by positron annihilation lifetime spectroscopy. *J Membr Sci* 2018;549:581–7.
- [13] Usman A, Hussain Z, Riaz A, Khan AN. Enhanced mechanical, thermal and antimicrobial properties of poly (vinyl alcohol)/graphene oxide/starch/silver nanocomposites films. *Carbohydr Polym* 2016;153:592–9.
- [14] Soliman TS, Vshivkov SA, Elkalashy SI. Structural, linear and nonlinear optical properties of Ni nanoparticles – polyvinyl alcohol nanocomposite films for optoelectronic applications. *Opt Mater* 2020;107:110037.
- [15] Yang X, Guo Y, Han Y, Li Y, Ma T, Chen M, et al. Significant improvement of thermal conductivities for BNNS/PVA composite films via electrospinning followed by hot-pressing technology. *Compos B Eng* 2019;175:107070.
- [16] Liang X, Niu C-G, Zhang L, Wen X-J, Yang S-F, Guo H, et al. Construction of 2D heterojunction system with enhanced photocatalytic performance: plasmonic Bi and reduced graphene oxide co-modified Bi₅O₇I with high-speed charge transfer channels. *J Hazard Mater* 2019;361:245–58.
- [17] Sharma G, Dionysiou DD, Sharma S, Kumar A, Ala'a H, Naushad M, et al. Highly efficient Sr/Ce/activated carbon bimetallic nanocomposite for photoinduced degradation of rhodamine B. *Catal Today* 2019;335:437–51.
- [18] Gao X, Li R, Hu L, Lin J, Wang Z, Yu C, et al. Preparation of boron nitride nanofibers/PVA composite foam for environmental remediation. *Colloids Surf A Physicochem Eng Asp* 2020;604:125287.
- [19] Waldron RD. Infrared spectra of ferrites. *Phys Rev* 1955;99:1727–35.
- [20] White WB, DeAngelis BA. Interpretation of the vibrational spectra of spinels. *Spectrochim Acta Part A Mol Spectrosc* 1967;23:985–95.
- [21] Ateia E, Salah LM, El-Bassuony AAH. Investigation of cation distribution and microstructure of nano ferrites prepared by different wet methods. *J Inorg Organomet Polym Mater* 2015;25:1362–72.
- [22] Datt G, Kotabage C, Datar S, Abhyankar AC. Correlation between the magnetic-microstructure and microwave mitigation ability of M_xCo(1-x)Fe₂O₄ based ferrite-carbon black/PVA composites. *Phys Chem Chem Phys* 2018;20:26431–42.
- [23] Mustaqeem M, Saleh TA, ur Rehman A, Farooq Warsi M, Mehmood A, Sharif A, et al. Synthesis of Zn_{0.8}Co_{0.1}Ni_{0.1}-Fe₂O₄ polyvinyl alcohol nanocomposites via ultrasound-assisted emulsion liquid phase. *Arab J Chem* 2020;13:3246–54.
- [24] Khairy M. Synthesis, characterization, magnetic and electrical properties of polyaniline/NiFe₂O₄ nanocomposite. *Synth Met* 2014;189:34–41.
- [25] Shaopu L. A highly sensitive colour reaction for Se(IV) with the iodide-rhodamine B-PVA system Spectrophotometric determination of trace amounts of selenium in water. *Talanta* 1990;37:749–52.
- [26] Fernandes DM, Hechenleitner AAW, Lima SM, Andrade LHC, Caires ARL, Pineda EAG. Preparation, characterization, and photoluminescence study of PVA/ZnO nanocomposite films. *Mater Chem Phys* 2011;128:371–6.
- [27] Le KQ, Dang NH. Photoluminescence Spectroscopy of Rhodamine 800 aqueous solution and dye-doped polymer thin-film: concentration and solvent effects. *J Electron Mater* 2018;47:4813–7.
- [28] Zhao X, Wang A, Gao S, Yan D, Guo W, Xu Y, et al. Enhancing photoluminescence of carbon quantum dots doped PVA films with randomly dispersed silica microspheres. *Sci Rep* 2020;10:5710.
- [29] Ali ZI, Hosni HM, Saleh HH, Ghazy OA. Photoluminescence and electrical properties of polyvinyl alcohol films doped with CdS nanoparticles. *Appl Phys A* 2016;122:5. <https://doi.org/10.1007/s00339-016-0037-4>.